ICREN-01/2013 February 16-17, 2013 Constantine, Algeria
First International Conference on Renewable Energies and Nanotechnology impact on Medicine and Ecology

Numerical Study of the Mixed Convection Heat Transfer Enhancement by Using of the Longitudinal and Transversal Internal Fins in a Heated Horizontal Pipe

Sofiane Touahri, Toufik Boufendi*

Energy Physics Laboratory, Physics Department, University of Constantine I, 25000, Algeria

Abstract

In this work, we numerically study the three-dimensional mixed convection heat transfer in a horizontal pipe equipped by longitudinal and transversal attached fins on its internal surface for the solar application such as the water or air heating with solar panel. The pipe and fins are heated by an electrical intensity passing through their small thickness. The longitudinal fins studied number is: 2 vertical, 4 and 8 fins, while the number of transversal fins is 8 fins. The considered heights fin are H=0.12 cm and H=0.24 cm. The convection in the fluid domain is conjugated to thermal conduction in the pipe and fins solid thickness. The physical properties of the fluid are thermal dependant. The heat losses from the external pipe surface to the surrounding ambient are considered. The model equations of continuity, momenta and energy are numerically solved by a finite volume method with a second order spatiotemporal discretization. As expected for the longitudinal fins, the axial Nusselt number increase with increasing of number and height of fins. For Gr= 5.1 10^5, the average Nusselt number without fins is equal to 13.144. The introduce of longitudinal fins gives an average Nusselt number equal to 16.83, 22.523 and 32.066 for 2 vertical, 4 and 8 fins respectively. The participation of fins located in the lower part of the tube on the improvement of heat transfer is higher than the participation of the upper fins. On the other hand, the longitudinal fins participate directly on increase of the heat transfer; this is justified by the large local Nusselt number along the interface of the fins. This participation is moderate in the case of transverse fins, these latter are used to mix the fluid for increased the local Nusselt number to the interface in the cylindrical axial sections following the transversal fins.

Keywords : Conjugate Heat Transfer; Mixed Convection; Internal Fins; Numerical simulation.

Nomenclature

D_e, D_i	external and internal pipe diameter respectively, [m]
Gr^*	modified Grashof number $(= g\beta G D_i^5 / K_s \nu^2)$, [–]
G^*	non-dimensional volumetric heat generation $(= K_s^* / Re_0 \, Pr_0)$, [–]
H	height of the fin, [m]

h_c, h_r	convective and radiative local heat transfer coefficients respectively, [$Wm^{-2}K^{-1}$]
K^*	non-dimensional thermal conductivity, $(= K / K_0)$, [–]
L^*	non-dimensional pipe length ($= L / D_i$), [–]
Nu(θ, z)	local Nusselt number ($= h(\theta, z) D_i / K_0$), [–]
P^*	non-dimensional pressure $(=(P - P_0) / \rho_0 V_0^2)$, [–]
Pr	Prandtl number ($= \nu/\alpha$), [–]
q	heat flux, [W m^{-2}]
r^*	non-dimensional radial coordinate ($= r / D_i$), [–]
R	pipe radius, [m]
Re	Reynolds number ($= V_0 D_i / v_0$), [–]
t^*	non-dimensional time ($= V_0 t / D_i$), [–]
T^*	non-dimensional temperature $(=(T - T_0)/(G D_i^2 / K_s))$, [–]
T_b^*	non-dimensional mixing cup section temperature, $(=(T_b - T_0)/(G D_i^2/K_s))$, [–]
V_0	mean axial velocity at the pipe entrance, [m s^{-1}]
V_r, V_θ, V_z	radial, circumferential and axial velocities components, respectively, [m s^{-1}]
V_r^*, V_θ^*, V_z^*	non-dimensional velocities components, ($= V_r / V_0, V_\theta / V_0, V_z / V_0$), [–]
z , z^*	axial and non-dimensional axial coordinate respectively, ($= z / D_i$), [–]
Greek symbols	
α	thermal diffusivity, [$m^2 s^{-1}$]
β	thermal expansion coefficient, [K^{-1}]
μ	dynamic viscosity, [kg m s^{-1}]
μ^*	non-dimensional dynamic viscosity ($= \mu / \mu_0$), [–]
θ	angular coordinate, [rad]
ρ	density, [kgm^{-3}]
σ	the Stephan-Boltzmann constant (= 5.67 10^{-8}), [$Wm^{-2}K^{-4}$]
τ	stress, [Nm^{-2}]
τ^*	non-dimensional stress $(= \tau / (\mu_0 V_0 / D_i))$, [–]

1. Introduction

Finned tubes are often used in many engineering sectors for extend the contact surface between the tube wall and the fluid and improve the heat transfer; the researchers have studied the problem of

* T. Boufendi. Tel.:+213.771794491; fax:+213.31818872.
boufendit@yahoo.fr; tboufendi@umc.edu.dz

optimizing the shape and geometry of attached fins in order to increase heat transfer effectiveness. Most of the studies performed on this optimization consider longitudinal fins which have symmetrical lateral profiles; this assumption simplifies the treatment of the problem with regard to the boundary conditions and gives symmetrical results concerning velocity and temperature profiles. Many investigations, both experimental and numerical, have been conducted for different kinds of internally finned tubes. **Patankar et al.[1]**, presented an analytical model for fully developed turbulent air flow in internally finned tubes and annuli. In their study, the longitudinal attached fins in the inner wall were considered. The thermal boundary conditions were constant heat flux at the inner surface, the results of this study consisted of heat transfer and pressure drop coefficients. A combined numerical and experimental study of plate-fin and tube heat exchangers was examined by **Jang et al. [2]**. In their study, the detailed numerical results of pressure drop and heat transfer coefficient are presented. **Alam et al. [3]** conducted a numerical study on hydrodynamically fully developed, thermally developing flow inside circular tubes with internal longitudinal fins having tapered lateral profiles. The results showed significant heat transfer enhancement with the inclusion of internal fins. Water and engine oil were assumed as fluids in their numerical studies, and they concluded water to be a better coolant as compared to engine oil. **Dong et al. [4]** conducted a numerical study of thermally developing flow in an elliptical duct with four longitudinal internal fins of zero thickness. A control volume based on finite difference technique was used in the numerical analysis and an optimum value of the local Nusselt number was obtained as a function of the fin height. **Huq et al. [5]** performed an experimental analysis of heat transfer in an internally finned tube, the experimental results were compared with results from the smooth channel tube, and a significant improvement in heat transfer was observed for internally finned cases. Similar studies were also examined experimentally by **Wei-Mon Yan et al. [6], B. Yu et al. [7] and Wang et al. [8].**

In this work, we studied numerically the heat transfer by mixed convection in horizontal pipe equipped by longitudinal and transversal attached fins on its internal wall. The mixed convection is conjugate with thermal conduction in the pipe and fins walls. The physical properties of the fluid are thermo- dependent and the heat losses with the external environment are considered. The objective of our work is study the enhancement gives to the heat transfer by using different fins shape.

2. The geometry and mathematical model

Figure 1 illustrates the problem geometry. We consider a long horizontal pipe having a length L=1m, an inside diameter D_i=0.96cm and an external diameter D_o=1cm, this later is equipped by longitudinal and transversal attached fins on its internal surface.

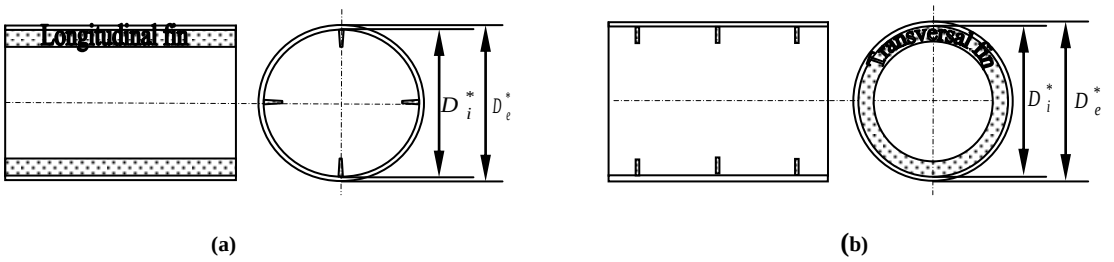

Fig. 1. (a) Longitudinal fin; **(b)** Transversal fin

The longitudinal fins are fixed at (θ=0), (θ=π/4), (θ=π/2), (θ=3π/4), (θ=π), (θ=5π/4), (θ=3π/2) and (θ=7π/4) while the transversal fins are attached at z^*=9.4404, z^*=19.8574, z^*=30.2744, z^*=40.6914, z^*=51.1084, z^*=61.5254, z^*=75.8488 and z^*=82.3594. The pipe and fins is made of Inconel having a

thermal conductivity K_s = 20 W/m K. An electric current passing along the pipe (in the solid thickness) produced a heat generation by the Joule effect. This heat is transferred to distilled water flow in the pipe. At the entrance the flow is of Poiseuille type with an average axial velocity equal to 7.2 10^{-2} m/s and a constant temperature of 15 °C. The density is a linear function of temperature and the Boussinesq approximation is applied.

The physical principles involved in this problem are well modeled by the following non dimensional conservation partial differential equations with their initial and boundary conditions:

At $t^* = 0$:

$$V_r^* = V_\theta^* = V_z^* = T^* = 0 \tag{1}$$

At $t^* > 0$:

– Mass conservation equation:

$$\frac{1}{r^*}\frac{\partial}{\partial r^*}\left(r^* V_r^*\right) + \frac{1}{r^*}\frac{\partial V_\theta^*}{\partial \theta} + \frac{\partial V_z^*}{\partial z^*} = 0 \tag{2}$$

– Radial momentum conservation equation:

$$\frac{\partial V_r^*}{\partial t^*} + \frac{1}{r^*}\frac{\partial}{\partial r^*}\left(r^* V_r^* V_r^*\right) + \frac{1}{r^*}\frac{\partial}{\partial \theta}\left(V_\theta^* V_r^*\right) + \frac{\partial}{\partial z^*}\left(V_z^* V_r^*\right) - \frac{V_\theta^{*2}}{r^*} =$$
$$-\frac{\partial P^*}{\partial r^*} + \frac{Gr_0^*}{\mathrm{Re}_0^2}\cos\theta\, T^* + \frac{1}{\mathrm{Re}_0}\left[\frac{1}{r^*}\frac{\partial}{\partial r^*}\left(r^* \tau_{rr}^*\right) + \frac{1}{r^*}\frac{\partial}{\partial \theta}\left(\tau_{r\theta}^*\right) - \frac{\tau_{\theta\theta}^*}{r^*} + \frac{\partial}{\partial z^*}\left(\tau_{rz}^*\right)\right] \tag{3}$$

– Angular momentum conservation equation:

$$\frac{\partial V_\theta^*}{\partial t^*} + \frac{1}{r^*}\frac{\partial}{\partial r^*}\left(r^* V_r^* V_\theta^*\right) + \frac{1}{r^*}\frac{\partial}{\partial \theta}\left(V_\theta^* V_\theta^*\right) + \frac{\partial}{\partial z^*}\left(V_z^* V_\theta^*\right) + \frac{V_r^* V_\theta^*}{r^*} =$$
$$-\frac{1}{r^*}\frac{\partial P^*}{\partial \theta} - \frac{Gr_0^*}{\mathrm{Re}_0^2}\sin\theta\, T^* + \frac{1}{\mathrm{Re}_0}\left[\begin{array}{l}\frac{1}{r^{*2}}\frac{\partial}{\partial r^*}\left(r^{*2}\tau_{\theta r}^*\right) + \\ \frac{1}{r^*}\frac{\partial}{\partial \theta}\left(\tau_{\theta\theta}^*\right) + \frac{\partial}{\partial z^*}\left(\tau_{\theta z}^*\right)\end{array}\right] \tag{4}$$

– Axial momentum conservation equation:

$$\frac{\partial V_z^*}{\partial t^*} + \frac{1}{r^*}\frac{\partial}{\partial r^*}\left(r^* V_r^* V_z^*\right) + \frac{1}{r^*}\frac{\partial}{\partial \theta}\left(V_\theta^* V_z^*\right) + \frac{\partial}{\partial z^*}\left(V_z^* V_z^*\right) =$$
$$-\frac{\partial P^*}{\partial z^*} + \frac{1}{\mathrm{Re}_0}\left[\frac{1}{r^*}\frac{\partial}{\partial r^*}\left(r^* \tau_{rz}^*\right) + \frac{1}{r^*}\frac{\partial}{\partial \theta}\left(\tau_{\theta z}^*\right) + \frac{\partial}{\partial z^*}\left(\tau_{zz}^*\right)\right] \tag{5}$$

– Energy conservation equation:

$$\frac{\partial T^*}{\partial t^*} + \frac{1}{r^*}\frac{\partial}{\partial r^*}\left(r^* V_r^* T^*\right) + \frac{1}{r^*}\frac{\partial}{\partial \theta}\left(V_\theta^* T^*\right) + \frac{\partial}{\partial z^*}\left(V_z^* T^*\right) = G^* - \frac{1}{\mathrm{Re}_0 \mathrm{Pr}_0}\left[\begin{array}{l}\frac{1}{r^*}\frac{\partial}{\partial r^*}\left(r^* q_r^*\right) + \\ \frac{1}{r^*}\frac{\partial}{\partial \theta}\left(q_\theta^*\right) + \frac{\partial}{\partial z^*}\left(q_z^*\right)\end{array}\right] \tag{6}$$

where $G^* = \begin{cases} K_S^* / \left(\mathrm{Re}_0 \, \mathrm{Pr}_0\right) & \textit{in the solid} \\ 0 & \textit{in the fluid} \end{cases}$

The viscous stress tensor components are:

$$\tau_{rr}^* = 2\mu^* \frac{\partial V_r^*}{\partial r^*} \qquad \tau_{r\theta}^* = \tau_{\theta r}^* = \mu^* \left[r^* \frac{\partial}{\partial r^*}\left(\frac{V_\theta^*}{r^*}\right) + \frac{1}{r^*}\frac{\partial V_r^*}{\partial \theta} \right]$$

$$\tau_{\theta\theta}^* = 2\mu^* \left[\frac{1}{r^*}\frac{\partial V_\theta^*}{\partial \theta} + \frac{V_r^*}{r^*} \right] \qquad \tau_{\theta z}^* = \tau_{z\theta}^* = \mu^* \left[\frac{\partial V_\theta^*}{\partial z^*} + \frac{1}{r^*}\frac{\partial V_z^*}{\partial \theta} \right]$$

$$\tau_{zz}^* = 2\mu^* \frac{\partial V_z^*}{\partial z^*} \qquad \tau_{zr}^* = \tau_{rz}^* = \mu^* \left[\frac{\partial V_z^*}{\partial r^*} + \frac{\partial V_r^*}{\partial z^*} \right] \tag{7}$$

The heat fluxes are:

$$q_r^* = -K^* \frac{\partial T^*}{\partial r^*} \quad , \quad q_\theta^* = -\frac{K^*}{r^*}\frac{\partial T^*}{\partial \theta^*} \quad \textit{and} \quad q_z^* = -K^* \frac{\partial T^*}{\partial z^*} \tag{8}$$

2.1 The boundary conditions

The previous differential equations are solved with the following boundary conditions:

At the pipe entrance: $z^* = 0$

– In the fluid domain:

$0 \le r^* \le 0.5$ and $0 \le \theta \le 2\pi$:

$$V_r^* = V_\theta^* = T^* = 0 \, , V_z^* = 2\left(1 - 4r^{*2}\right) \tag{9}$$

– In the solid domain:

$0.5 \le r^* \le 0.5208$ and $0 \le \theta \le 2\pi$:

$$V_r^* = V_\theta^* = V_z^* = T^* = 0 \tag{10}$$

At the pipe exit: $z^* = 104.17$

– In the fluid domain:

$0 \le r^* \le 0.5$ and $0 \le \theta \le 2\pi$:

$$\frac{\partial V_r^*}{\partial z^*} = \frac{\partial V_\theta^*}{\partial z^*} = \frac{\partial V_z^*}{\partial z^*} = \frac{\partial}{\partial z^*}\left(K^* \frac{\partial T^*}{\partial z^*} \right) = 0 \tag{11}$$

– In the solid domain:

$0.5 \le r^* \le 0.5208$ and $0 \le \theta \le 2\pi$:

$$V_r^* = V_\theta^* = V_z^* = \frac{\partial}{\partial z^*}\left(K^* \frac{\partial T^*}{\partial z^*}\right) = 0 \tag{12}$$

At the outer wall: $r^* = 0.5208$

The conductive heat flux is equal to the sum of the heat fluxes of the radiation and natural convection losses.

for $0 \leq \theta \leq 2\pi$ and $0 \leq z^* \leq 104.17$

$$\begin{cases} V_r^* = V_\theta^* = V_z^* = 0 \\ -K^* \dfrac{\partial T^*}{\partial r^*} = \dfrac{(h_r + h_c) D_i}{K_0} T^* \end{cases} \tag{13}$$

where:

$$h_r = \varepsilon \sigma \left(T^2 + T_\infty^2\right)\left(T + T_\infty\right) \tag{14}$$

The emissivity of the outer wall ε is arbitrarily chosen to 0.9 while h_c is derived from the correlation of Churchill and Chu [9] valid for all Pr and for Rayleigh numbers in the range $10^{-6} \leq \mathrm{Ra} \leq 10^9$.

$$Nu = \left[h_c D_i / K_{air}\right] = \left[0.6 + \left(0.387\, Ra^{1/6} / \left(1 + \left(0.559 / \mathrm{Pr}_{air}\right)^{9/16}\right)^{8/27}\right)\right]^2 \tag{15}$$

The Rayleigh and the Prandtl numbers defined, respectively, as:

$$Ra = \frac{g\beta \left[T(R_o, \theta, z) - T_\infty\right] D_o^3}{\alpha_{air} \nu_{air}}, \quad Pr_{air} = \nu_{air} / \alpha_{air} \tag{16}$$

In this expressions of the Rayleigh and the Prandtl numbers the thermophysical properties of the air ambient are evaluated at the local film temperature given as: $T_{film} = \left[T(R_o, \theta, z) + T_\infty\right]/2$.

In this matter, the used concept of the conjugate heat transfer problem, discussed in Patankar [10], consists in considering the same field of work for the fluid and solid domains. This is evident for the fluid domain, but for the solid domain this is obtained by imposing an infinite viscosity to the fluid. In our calculations we have considered the solid as a fluid with a dynamic viscosity equal to 10^{30}. This very large viscosity within the solid domain ensures that the velocity of this part remains null and consequently the heat transfer is only by conduction deducted from the eq. (6).

2.2 The Nusselt numbers

At the cylindrical solid-fluid interface, the local Nusselt number is defined as:

$$Nu(\theta, z^*) = \frac{h(\theta, z^*) D_i}{K_0} = \left[\frac{\left(K^* \partial T^* / \partial r^*\right)_{r^* = 0.5}}{T^*(0.5, \theta, z^*) - T_b^*(z^*)}\right] \tag{17}$$

The axial Nusselt number for the cylindrical interface is defined as:

$$Nu(z^*) = \frac{1}{2\pi} \int_0^{2\pi} Nu(\theta, z^*)\, d\theta \tag{18}$$

Finally, we can define an average Nusselt number for the whole cylindrical solid-fluid interface:

$$Nu_A = \frac{1}{(2\pi)(104.17)} \int_0^{2\pi} \int_0^{104.17} Nu(\theta, z^*)\, dz^*\, d\theta \tag{19}$$

At the longitudinal fin interface, the local Nusselt number is defined as:

$$Nu(r^*, z^*) = \frac{h(r^*, z^*) D_h}{K_0} = \left[\frac{\left(K^*/r^*\right)\left(\partial T^*/\partial\theta\right)\Big|_{\theta=\theta_{fin}}}{T^*(r^*, \theta_{fin}, z^*) - T_m^*(z^*)} \right] \tag{20}$$

The axial Nusselt number for the longitudinal fin interface is defined as:

$$Nu(z^*) = \frac{1}{H^*} \int_{R_i^* - H^*}^{R_i^*} Nu(r^*, z^*)\, dr^* = \frac{1}{H^*} \int_{R_i^* - H^*}^{R_i^*} \left[\frac{\left(K^*/r^*\right)\left(\partial T^*/\partial\theta\right)\Big|_{\theta=\theta_{fin}}}{T^*(r^*, \theta_{fin}, z^*) - T_m^*(z^*)} \right] dr^* \tag{21}$$

The average Nusselt number for the longitudinal fin interface is defined as:

$$Nu_A = \frac{1}{L^*} \int_0^{L^*} Nu(z^*)\, dz^* \tag{22}$$

At the transversal fin interface, the local Nusselt number is defined as:

$$Nu(r^*, \theta) = \frac{h(r^*, \theta) D_h}{K_0} = \left[\frac{\left(K^*\right)\left(\partial T^*/\partial z\right)\Big|_{z=z_{fin}}}{T^*(r^*, \theta, z^*_{fin}) - T_m^*(z^*)} \right] \tag{23}$$

The axial Nusselt number for the transversal fin interface is defined as:

$$Nu(z^*) = \frac{1}{(2\pi)H^*} \int_0^{2\pi} \int_{R_i^* - H^*}^{R_i^*} \left[\frac{\left(K^*\right)\left(\partial T^*/\partial z\right)\Big|_{z^*=z^*_{fin}}}{T^*(r^*, \theta, z^*_{fin}) - T_m^*(z^*)} \right] dr^*\, d\theta \tag{24}$$

3. The numerical method

For the numerical solution of modelling equations, we used the finite volume method well described by Patankar [10]; the using of this method involves the discretization of the physical domain into a discrete domain constituted of finite volumes where the modelling equations are discretized in a typical volume. We used a temporal discretization with a truncation error of $\left(\Delta t^*\right)^2$ order. The convective and nonlinear terms have been discretized according to the Adams-Bashforth numerical scheme, with a truncation error of $\left(\Delta t^*\right)^2$ order, the diffusive and pressure terms are implicit. Regarding the spatial discretization, we used the central differences pattern with a truncation error of $\left(\Delta r^*\right)^2, \left(\Delta\theta^*\right)^2$ and $\left(\Delta z^*\right)^2$ order. So our spatio-temporal discretization is second order. The mesh used contains 52×88×162 points in the radial, azimuthal and axial directions. The considered time step is $\Delta t^* = 5.10^{-4}$ and the time marching is pursued until the steady state is reached. The steady state is controlled by the satisfaction of the global mass and energy balances as well as the levelling off of the time evolution of the hydrodynamic and thermal fields.

4. Results and discussions

4.1 Development of the secondary flow

All the results presented in this paper were calculated for Reynolds number, Re = 606.85, and the Prandtl number, Pr=8.082, while the Grashof number is equal to 5.1 10^5. The obtained flow for the studied cases is characterized by a main flow along the axial direction and a secondary flow influenced by the density variation with temperature, which occurs in the plane $(r^* - \theta)$, this flows are presented for 8 fins in the case of longitudinal fins and 4 fins in the case of transversal fins.

In the reference case (forced convection) the transverse motion is inexistence, the only flow is in axial direction. In the presence of volumetric heating in the pipe and fins wall, a transverse flow exists and explained as follows: the hot fluid moves along the hot wall from the bottom of the outer tube $(\theta = \pi)$ upwards $(\theta = 0)$ and moves down from the top to the bottom along the centre of tube. The vertical plane passing through the angles $(\theta = 0)$ and $(\theta = \pi)$ is a plane of symmetry. The transverse flow in the $(\vec{r}, \theta)$ plane is represented by counter rotating cells; the cells number is proportional to longitudinal fins number. In figure 2, we present the secondary flow vectors at the pipe exit for the case of longitudinal fins. For the case of transversal fins, the position of fins is only in selected axial sections. Far from these sections, the secondary motion is similar to that of simple cylindrical pipe. In figure 3, we present the secondary flow vectors at the fourth transversal fin section (z^*=40.6914).

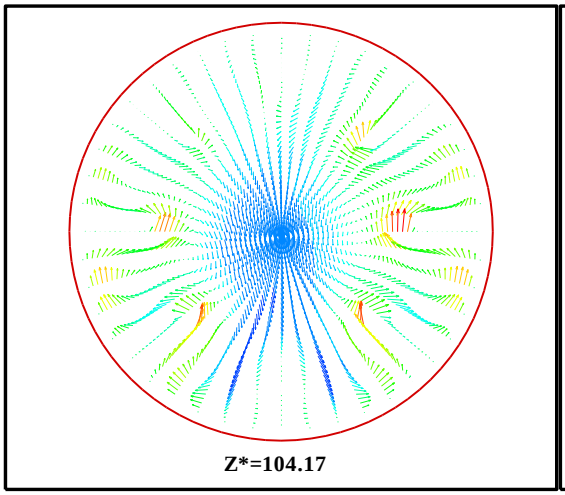

Fig. 2. Development of the secondary flow vectors at the pipe exit for longitudinal fins

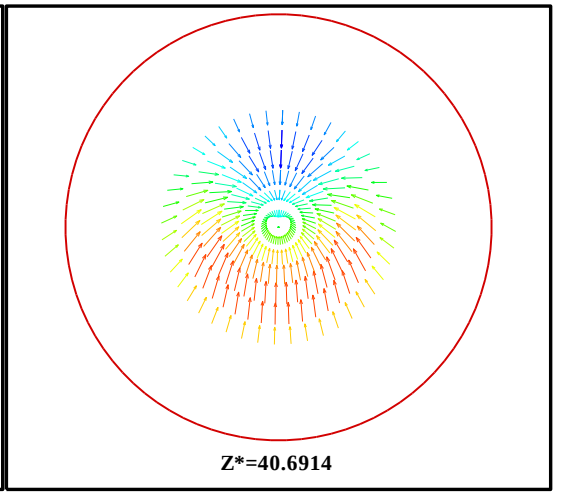

Fig. 3. Development of the secondary flow vectors at the fourth transversal fin section

4.2 Development of the axial flow

At the entrance, the axial flow is axisymmetric with the maximum velocity in the center of the pipe. In the presence of volumetric heating in the pipe and the fins walls, the configuration of the axial flow completely changes because the secondary flow causes an angular variation which has a direct influence on the distribution of axisymmetric axial flow. In figure 4, the axial flow is presented at the exit of the pipe for the case of longitudinal fins having height H^* equal to 0.1875. In figure 5, the axial flow is presented at the fourth transversal fin section (z^*=40.6914). Through these figures, it is clear that the axial velocity is zero in the fins walls.

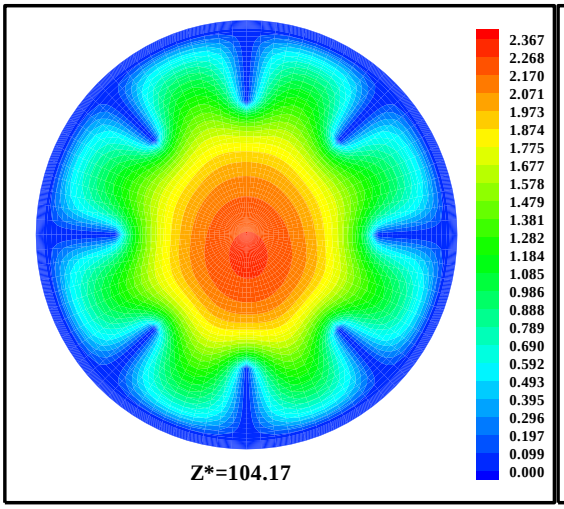

Fig. 4. Axial velocity profiles at the pipe exit for longitudinal fins

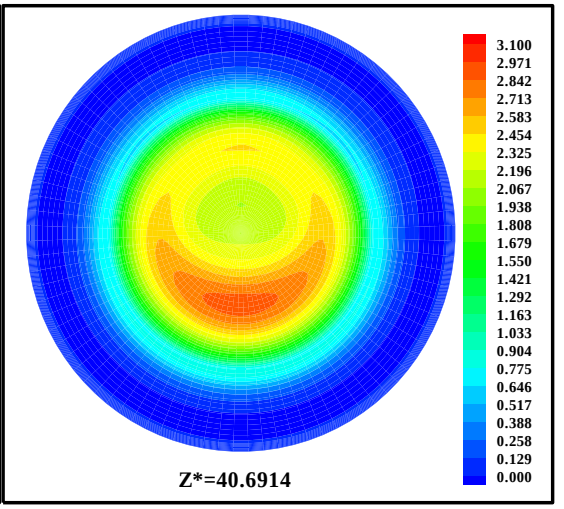

Fig. 5. Axial velocity profiles at the fourth transversal fin section

4.3 Development of the temperature field

In the presence of volumetric heating, a transverse flow exists and thus changes the axisymmetric distribution of fluid and gives it an angular variation, this variation explained as follows: the hot fluid near from the pipe and fins walls moves upwards under the buoyancy force effect, the relatively cold fluid descends down in de centre of the pipe.

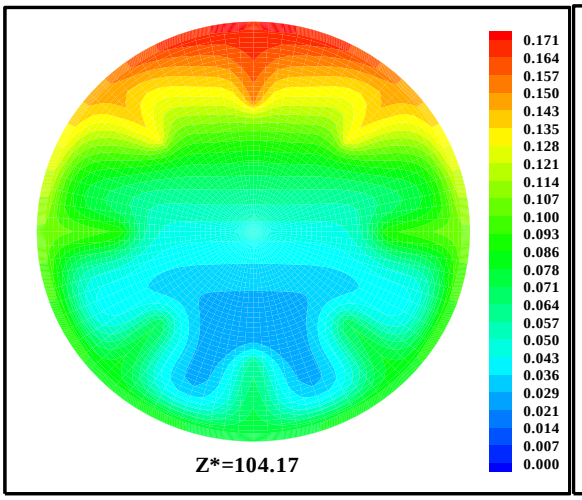

Fig. 6. The isotherms at the pipe exit for longitudinal fins

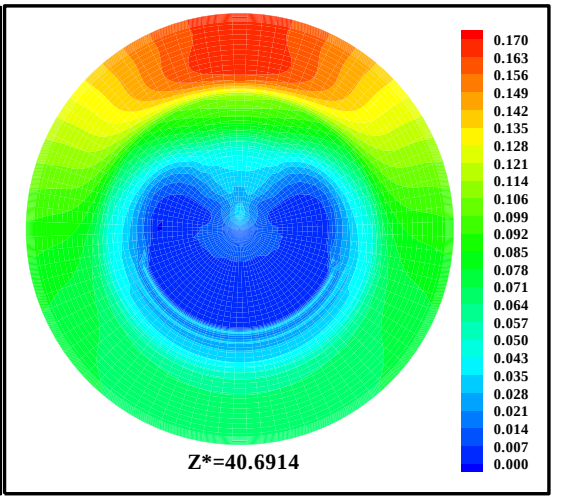

Fig. 7. The isotherms at the fourth transversal fin section

A permanent generation of heat in the pipe and the fins walls imposes a continuous increase of the temperature of the fluid up to the exit of the pipe. The obtained results show that at given section, the maximum fluid temperature T^* is all the time located at $r^* = 0.5$ and $\theta = 0$ (top of solid-fluid interface), because the hot fluid is driven by the secondary motion towards the top of the pipe. The isotherms are

presented at the exit of the pipe for the case of longitudinal fins having height H^* equal to 0.1875 in figure 6 and at the fourth transversal fin section (z^*=40.6914) in figure 7.

4.4 The Nusselt numbers

The phenomenon of heat transfer has been characterized in terms of Nusselt numbers calculated at the inner wall of the pipe, which is obtained by Eq (17) and those calculated at the fins wall, obtained by Eq (20) and (23). The variation of local Nusselt number at cylindrical interface is presented in figure 8 for the case of longitudinal fins and in figure 9 for the case of transversal fins.

The local Nusselt number of longitudinal fins placed in the right side of the pipe at (θ=0), (θ=π/4), (θ=π/2), (θ=3π/4) and (θ=π) is shown in figure 10. The local Nusselt number takes a maximum value equal to 63.56 on the fin placed at (θ=3π/4), z^*=104.17 and r^*=0.3841.

The comparison of axial Nusselt numbers between finned tube and smooth tube is shown in figure 11. Quantitatively, there is a large increase in the axial Nusselt when the number of fins is increased. At the exit of the pipe, the axial Nusselt number is equal to 15.79, 23.47, 31.34 and 47.31 for the cases: smooth tube, tow vertical fins, four fins and eight fins respectively. The average Nusselt numbers for these cases are 13.144, 16.830, 22.523 and 32.066.

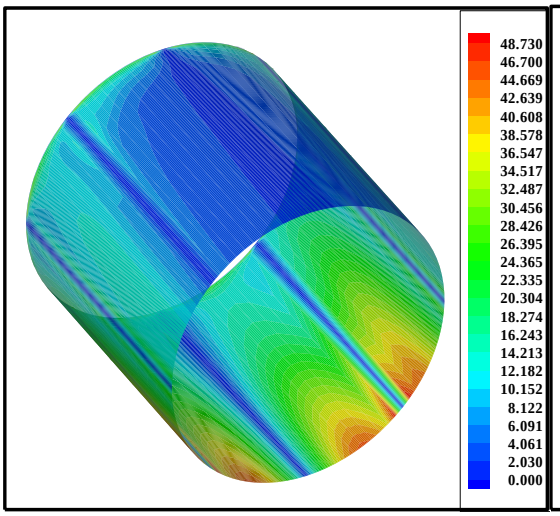

Fig. 8. The local Nusselt number variation at cylindrical interface for longitudinal fins case

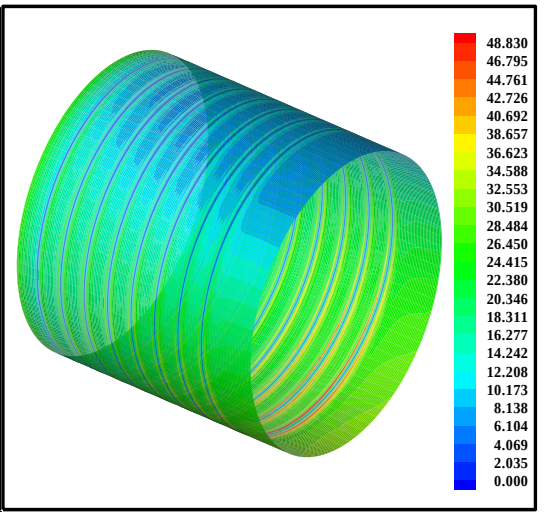

Fig. 9. The local Nusselt number variation at cylindrical interface for transversal fins case

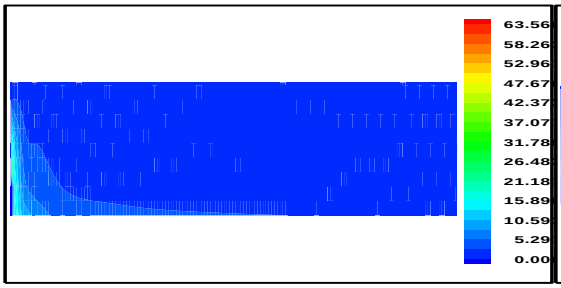

(a) Fin placed at (θ=0)

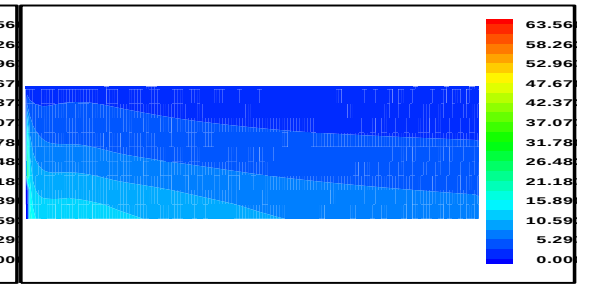

(b) Fin placed at (θ=π/4)

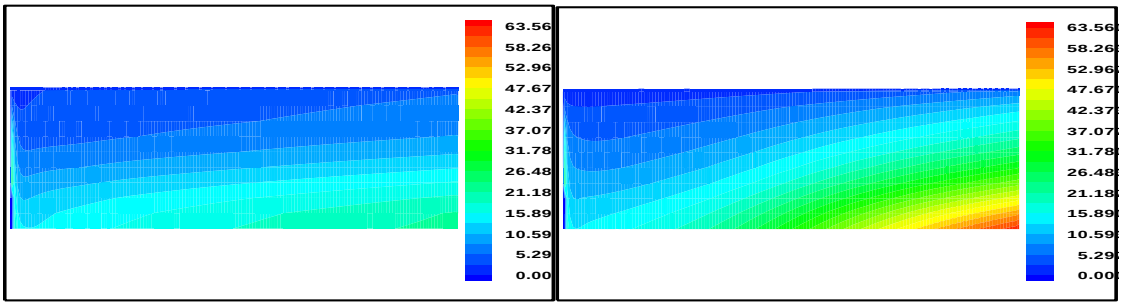

(c) Fin placed at (θ=π/2) (d) Fin placed at (θ=3π/4)

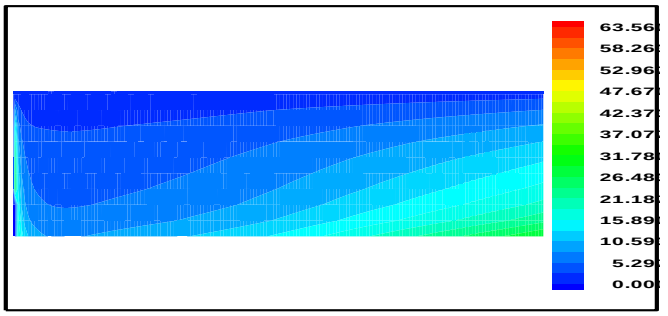

(c) Fin placed at (θ=π)

Fig. 10. The local Nusselt number variation at longitudinal fins interface

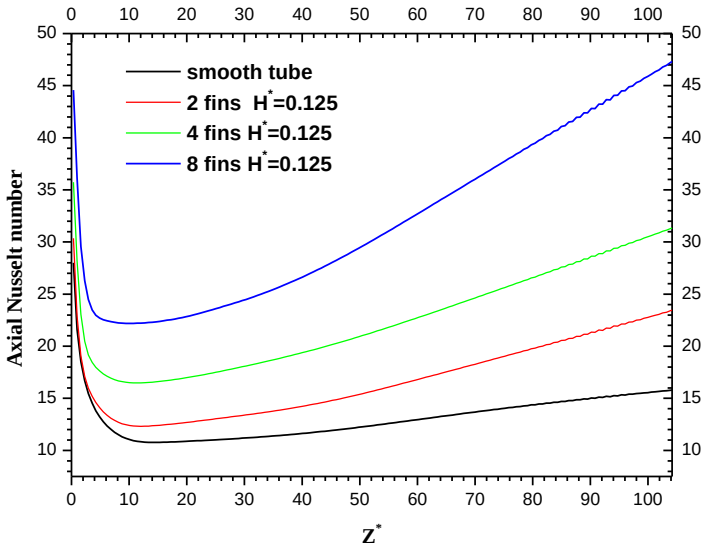

Fig. 11. Variation of axial Nusselt number for the different longitudinal fins studied cases

5. Conclusion

This study considers the numerical simulation of the three dimensional mixed convection heat transfer in a horizontal pipe equipped by longitudinal and transversal fins attached on its internal surface. The pipe and fins are heated by an electrical intensity passing through its small thickness. The obtained results show that the longitudinal fins participate directly in improving the heat transfer; this is justified by the high local Nusselt number at the interface of longitudinal fins. By cons, the transverse fins participate in an indirect way in improving the heat transfer their location facing the flow allowed to rearrange the structure of the fluid for each passage through the fins, which is used to mix the fluid and to increase the heat transfer to the cylindrical interfaces. The number and fins height are also important factors in improving the heat transfer.

References

[1] Patankar SV, Ivanovic M, Sparrow EM. Analysis of Turbulent Flow and Heat Transfer in Internally Finned Tubes and Annuli. *J. Heat Transfer, Vol.* 101, pp. 29-37, (1979).

[2] Jang JY, Wu MC, Chang WJ. Numerical and experimental studies of three-dimensional plate-fin and turbulent exchangers. *Int. J. Heat Mass Transfer, Vol.* 39, pp. 3057-3066, (1996).

[3] Alam I, Ghoshdastidar PS. A study of heat transfer effectiveness of circular tubes with internal longitudinal fins having tapered lateral profiles. *Int. J. Heat Mass Transfer, Vol.* 45 (6), pp. 1371–1376, (2002).

[4] Dong ZF, Ebadian MA. A numerical analysis of thermally developing flow in elliptical duct with internal fins. *Int. J. Heat Fluid Flo, Vol.* 12 (2), pp.166–172, (1991).

[5] Huq M, Huq AM, Rahman MM. Experimental measurements of heat transfer in an internally finned tube. *Int. Comm. Heat Mass Transfer. Vol.* 25 (5), pp. 619–630, (1998).

[6] Wei-Mon Yan, Pay-Jen Sheen. Heat transfer and friction characteristics of fin and tube heat exchangers. *International Journal of Heat and Mass Transfer, Vol.* 43, pp. 1651–1659, (2000).

[7] Yu B, Nie J H, Wang Q W, Tao W Q. Experimental study on the pressure drop and heat transfer characteristics of tubes with internal wave-like longitudinal fins, *Heat and Mass Transfer, Vol.* 35, pp. 65 –73, (1999).

[8] Wang CC, Fu W L, Chang CT. Heat transfer and friction characteristics of typical wavy fin and tube heat exchanger, *Exper. Thermal Fluid Science, Vol.* 14, pp. 174 – 186, (1997).

[9] Churchill SW, Chu HS. Correlating Equation for Laminar and Turbulent Free Convection from a Horizontal Cylinder, *International Journal of Heat and Mass Transfer, Vol.* 18, pp. 1049–1053, (1975).

[10] Patankar SV. *Numerical Heat Transfer and Fluid Flow,* McGraw-Hill, New-York, 1980.